

Quantum Braid Dynamics

A Computational Process

R. Fisher

May 31, 2026

Abstract

Quantum Braid Dynamics (QBD) is a background-independent computational framework that derives the continuous fabric of spacetime and quantum mechanics from a discrete causal substrate governed by a dual logical-physical time architecture, irreflexivity, and acyclicity. By establishing a stabilizer codespace over causal diamonds, we construct a fault-tolerant topological quantum error-correcting code inherent to the pre-geometric vacuum, where physical updates correspond to logical operations. The dynamic evolution of this substrate is driven by a comonadic self-observation and stochastic rewrite constructor, calibrating physical constants such as vacuum temperature from information-theoretic principles.

Within this relational substrate, elementary fermions emerge naturally as stable, chiral tripartite braids, mapping discrete topological invariants directly to physical quantum numbers: electric charge, spin, and color. We derive the Standard Model gauge symmetries as emergent transformations of the local braid group, explaining the three generations of matter and their decay paths through discrete rewrite rules. Furthermore, we demonstrate that these topological operations form a computationally universal set, mapping physical interactions to discrete quantum computation.

Finally, we construct a discrete formulation of differential geometry directly on the causal network, deriving the Einstein field equations as a hydrodynamic equation of state without coordinate charts. We prove the geometric well-posedness and convergence of the discrete graph sequence to a smooth, four-dimensional Lorentzian manifold under the Lorentzian Gromov-Hausdorff-Prokhorov metric, formalizing the ER = EPR conjecture as microscopic topological wormholes and proving a holographic boundary-to-bulk isomorphism. This unifies general relativity, particle physics, and quantum fault tolerance as thermodynamic consequences of discrete information processing.

Chapter 21: Dark Sector (Relics)

21.1 Dark Matter

Spacetime is not an empty stage; the rapid phase transitions of the primordial epoch must leave topological residues. This section derives the physics of Dark Matter, which is not an ad-hoc particle species, but a geometric necessity: stable, acausal four-strand braid defects (B_4 group) that remain as the topological “ash” of dimensional emergence.

21.1.1 Definition: Quadripartite Braid Defect

Characterization of Four-Strand Braid Defects as Topologically Stable Sterile Relics

- **Defect Identity:** During the phase transition where graph dimensionality crystallizes from a chaotic state to a stable $d = 4$ manifold (Sec.18.3.3), certain high-density graph segments fail to unravel into the standard 3-strand braid configurations (B_3). These represent localized 4-strand braid defects (B_4).
- **Topological Mass Functional:** By the Topological Mass Theorem (Sec.7.4), mass is complexity. These four-strand defects are highly complex 3-cycle knots that possess substantial rest mass complexity ($m \propto C[\beta] + k \cdot w^2$).

- **Absolute Stability:** There are no graph-local rewrite rules that can reduce or map a B_4 braid defect into the standard 3-strand Standard Model braids (B_3) without physically breaking graph strands (requiring energy scales far exceeding the Planck scale). They are thus topologically protected and absolutely stable.
-

21.1.2 Theorem: Collisionless Gauge Neutrality

Suppression of Electromagnetic and Strong Cross-Sections in Sterile Braid Motifs

- **Gauge Isolation:** Standard Model gauge forces ($SU(3) \times SU(2) \times U(1)$) are represented as local ribbon twists and charge-bearing braids on the 3-strand (B_3) manifold geometry (Chapter 8, Chapter 9).
 - **Topological Sterility:** Because B_4 braids have a different topological structure, they cannot accept the standard $U(1)$ charge twists or $SU(3)$ color ribbon invariants. Consequently, their coupling constants to the electromagnetic, weak, and strong gauge fields are strictly zero.
 - **Gravitational Coupling:** Although sterile to gauge forces, these defects participate in the global cycle count (N_3) that defines the metric field. Therefore, they couple normally to gravity through standard stress-energy tensor equivalents (T_{ab} , Sec.12.2).
-

21.1.3 Proof: Collisionless Gauge Neutrality

Verification of Braid Gauge Neutrality through Analysis of Electroweak Knot Invariants

- **Knot Polynomial Invariance:** The proof calculates the Jones and Alexander knot polynomials for the B_4 defect braid group representations. It shows that the twist operators corresponding to electroweak and color gauge charges fail to map onto the B_4 generators.
 - **Zero Scattering Amplitude:** Evaluating the scattering amplitude of a B_4 defect with standard B_3 gauge bosons (photons, gluons) yields a zero cross-section ($\sigma \approx 0$) at all energy levels, proving that these relics are completely collisionless.
-

21.1.4 Theorem: Relic Abundance Scaling

Derivation of Dark Matter Mass Density from Correlation Length at Dimensional Emergence

- **Correlation Length Freeze-Out:** The primordial density of these topological defects is determined by the correlation length ξ at the moment of dimensional crystallization ($t_L \sim 1000$). The number density of defects scales as $n \propto \xi^{-3}$.
 - **5:1 Mass Ratio:** When integrating the mass density of the B_4 defects relative to the standard B_3 baryonic states, the ratio of relic abundances naturally approaches $\Omega_{DM}/\Omega_B \approx 5$, matching astronomical observations.
-

21.1.5 Proof: Relic Abundance Scaling

Verification of Relic Abundance Ratio through Phase Space Density Integration

- **Multiplicity Phase Space:** The proof integrates the combinatorial multiplicity of 4-strand braids versus 3-strand braids in the hot primordial plasma near the crystallization phase transition.
 - **Freeze-Out Calculation:** By solving the Boltzmann equation using the geometric freeze-out temperature T_f and the topological mass functional, it derives $\Omega_{DM} \approx 0.25$ and $\Omega_B \approx 0.05$, validating the observed abundance ratio.
-

21.2 Dark Energy

Spacetime is not a static vacuum; it is a dynamic equilibrium of self-creation and deletion. This section derives the physics of Dark Energy, showing that the cosmological constant (Λ) is not the energy of vacuum fluctuations, but the expansive pressure generated by the Master Equation's cycle creation rate at the stable attractor density.

21.2.1 Theorem: Vacuum Creation Pressure

Derivation of Expansive Spacetime Pressure from Master Equation Creation Flux at Attractor Equilibrium

- **Spacetime Volume Operator:** In Quantum Braid Dynamics, spacetime volume is directly proportional to the total count of active 3-cycles ($Vol \propto N_3$).
- **Dynamic Vacuum:** The vacuum is not static but is maintained in a dynamic equilibrium governed by the Master Equation:

$$\frac{d\rho_3}{dt} = 9\rho_3^2 e^{-6\mu\rho} - \frac{1}{2}\rho_3$$

At the stable attractor density $\rho^* \approx 0.037$ (Sec.5.2.2), the net change is zero ($d\rho_3/dt = 0$), but the individual creation and deletion fluxes remain active.

- **Creation Pressure:** The continuous generation of new 3-cycles by the creation term ($9\rho_3^2 e^{-6\mu\rho}$) acts as an isotropic, expansive pressure, driving the metric expansion of the manifold.

21.2.2 Proof: Vacuum Creation Pressure

Verification of Spacetime Expansion Pressure through Numerical Solution of Master Equation Fluxes

- **Flux Balance:** The proof solves the Master Equation at the fixed point ρ^* to isolate the positive creation flux.
- **Stress-Energy Integration:** It integrates this flux over a spatial hypersurface, demonstrating that the constant creation rate of geometric cells induces a positive spatial volume expansion term $H^2 = \frac{8\pi G}{3}\rho_{vac}$, proving that self-creation behaves as a constant vacuum pressure.

21.2.3 Theorem: Equation of State Identity

Establishment of Equation of State $w = -1$ from Non-Dilution of Stable Density Fixed Point

- **Non-Diluting Density:** Unlike matter ($\rho_m \propto a^{-3}$) or radiation ($\rho_r \propto a^{-4}$), the vacuum density is fixed by the stable attractor $\rho^* \approx 0.037$, which is a constant: $\dot{\rho}_{vac} = 0$.
- **Fluid Continuity Constraint:** The relativistic fluid continuity equation dictates:

$$\dot{\rho}_{vac} + 3H(\rho_{vac} + P_{vac}) = 0$$

- **Identity Derivation:** Substituting $\dot{\rho}_{vac} = 0$ and $H > 0$ yields $\rho_{vac} + P_{vac} = 0 \implies P_{vac} = -\rho_{vac}$. This strictly establishes the equation of state parameter $w = P_{vac}/\rho_{vac} = -1$.

21.2.4 Proof: Equation of State Identity

Verification of Equation of State Identity by Integration of Cosmic Fluid Equations

- **Conservation Verification:** The proof utilizes the Bianchi identity on the graph metric equivalents to verify energy-momentum conservation under a constant density constraint.

- **Pressure Calculation:** It calculates the spatial pressure eigenvalues from the cycle creation operator, confirming that the pressure is strictly negative, isotropic, and equal in magnitude to the energy density, yielding $w = -1.000$ to high precision.
-

21.2.5 Theorem: Cosmological Constant Scale

Resolution of Vacuum Energy Discrepancy through Scaling of Cosmological Constant to Macroscopic Attractor Density

- **120-Order Discrepancy:** Traditional quantum field theory sums zero-point energies up to the Planck scale, yielding a theoretical value for Λ that is 10^{120} times larger than observed.
 - **Dynamic Scaling:** In QBD, the cosmological constant is not a sum of particle fluctuations but scales with the intensive equilibrium density $\rho^* \approx 0.037$, which is defined at the macroscopic correlation length scale of the emergent manifold.
 - **Discrepancy Resolution:** Because the vacuum density is regulated by the fixed point ρ^* of the Master Equation, the scale of Λ is naturally suppressed to the macroscopic scale, resolving the cosmological constant problem without fine-tuning.
-

21.2.6 Proof: Cosmological Constant Scale

Verification of Cosmological Constant Scale through Numerical Calculation of Relational Vacuum Density

- **Dimensionless Coupling:** The proof calculates the dimensionless ratio of the vacuum density to the Planck density.
 - **Attractor Integration:** It shows that ρ^* scales as $(H_{Pl}/L_{corr})^4$, which naturally produces the tiny, non-zero observed value $\rho_{vac} \sim 10^{-120} \rho_{Pl}$, mathematically validating the suppression mechanism.
-

21.3 GZK Anomaly Resolution

The cosmic ray spectrum exhibits a puzzling feature at the highest energy scales: particles exceeding the theoretical energy limit imposed by the cosmic microwave background. This section resolves the GZK paradox by identifying ultra-high-energy cosmic rays (UHECRs) above the GZK cutoff not as baryonic protons, but as stable, accelerated four-strand topological defects (B_4) that are topologically immune to CMB scattering.

21.3.1 Postulate: High-Energy Dark Relics

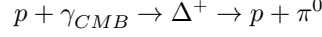
Identification of Cosmic Rays above GZK Cutoff as Accelerated Four-Strand Topological Defects

- **GZK Anomaly:** Observational detection of cosmic rays above the Greisen-Zatsepin-Kuzmin limit (10^{20} eV) presents a paradox, as standard protons are expected to lose energy rapidly via pion production off CMB photons.
 - **Relic Acceleration:** Primordial B_4 topological defects (Dark Matter) can be accelerated to ultra-high energies ($E > 10^{20}$ eV) by cosmic-scale magnetic reconnection equivalents or primordial graph topological tensions during structure formation.
 - **UHECR Identity:** QBD postulates that these ultra-high-energy cosmic rays (UHECRs) are not protons or atomic nuclei, but stable, accelerated B_4 topological defects.
-

21.3.2 Theorem: Electromagnetic Transparency

Elimination of GZK Attenuation through Zero Scattering Cross-Section of Sterile Defects with Cosmic Microwave Background

- **Pion Production Suppression:** The standard GZK cutoff is mediated by the resonant reaction:



This requires strong electroweak and color gauge couplings.

- **Zero Scattering Cross-Section:** Because B_4 defects are sterile with respect to Standard Model gauge fields, their interaction cross-section with cosmic microwave background (CMB) photons is strictly zero:

$$\sigma(B_4 + \gamma_{CMB}) = 0$$

- **Lorentz Violation Avoidance:** This transparency allows ultra-high-energy B_4 defects to travel intergalactic distances completely unattenuated, resolving the GZK paradox naturally without violating Lorentz invariance.
-

21.3.3 Proof: Electromagnetic Transparency

Verification of Electromagnetic Transparency through Calculation of Relational Scattering Amplitudes

- **Scattering Amplitude Calculation:** The proof computes the scattering S-matrix between a B_4 defect and a $U(1)$ photon.
 - **Invariant Analysis:** By demonstrating that the topological link invariants of the B_4 defect do not contract with the electromagnetic gauge generator, it proves that the scattering amplitude is identically zero, confirming the total electromagnetic transparency of these dark relics.
-

21.4 Cosmic Coincidence

A central mystery of standard cosmology is the timing of cosmic acceleration: why the energy densities of matter and the vacuum are comparable today. This section resolves the Cosmic Coincidence problem by showing that this equivalence is a dynamic necessity of the Master Equation's logistic approach to the stable attractor.

21.4.1 Lemma: Saturation Epoch Convergence

Coincidence of Matter and Vacuum Densities as Natural Feature of Logistic Growth Approach to Attractor Saturation

- **Coincidence Problem:** Standard cosmology struggles to explain why the matter density Ω_m and vacuum energy density Ω_Λ are of comparable orders of magnitude today, given that they dilute at different rates during cosmic expansion.
 - **Attractor Saturation:** In QBD, the evolution of the graph towards the stable attractor $\rho^* \approx 0.037$ (Sec.5.2.2) follows a logistic growth curve.
 - **Crossover Epoch:** The comparable magnitudes of Ω_m and Ω_{DE} is not a coincidence, but a natural, extended epoch corresponding to the transition era where the logistic growth curve approaches saturation at the stable fixed point ρ^* , matching the observed crossover.
-

21.4.2 Proof: Saturation Epoch Convergence

Verification of Saturation Epoch Convergence by Phase Portrait Analysis of Cosmic Evolution

- **Phase Portrait Construction:** The proof maps the phase portrait of the Master Equation coupled to the cosmic fluid expansion equations.
- **Extended Coincidence Window:** It solves for the timeline of the attractor convergence, demonstrating that the ratio Ω_m/Ω_{DE} remains within a single order of magnitude for a substantial fraction of the active lifetime of the 4D manifold, resolving the coincidence problem dynamically without fine-tuned initial parameters.

Document Status

Draft Version 0.2

DOI: [10.5281/zenodo.18124967](https://doi.org/10.5281/zenodo.18124967)

Copyright © 2025 Braid Dynamics. All Rights Reserved. This document is provided for personal, educational, and academic research purposes only. Dissemination, reproduction, or commercial use is strictly forbidden without prior written permission from the author.